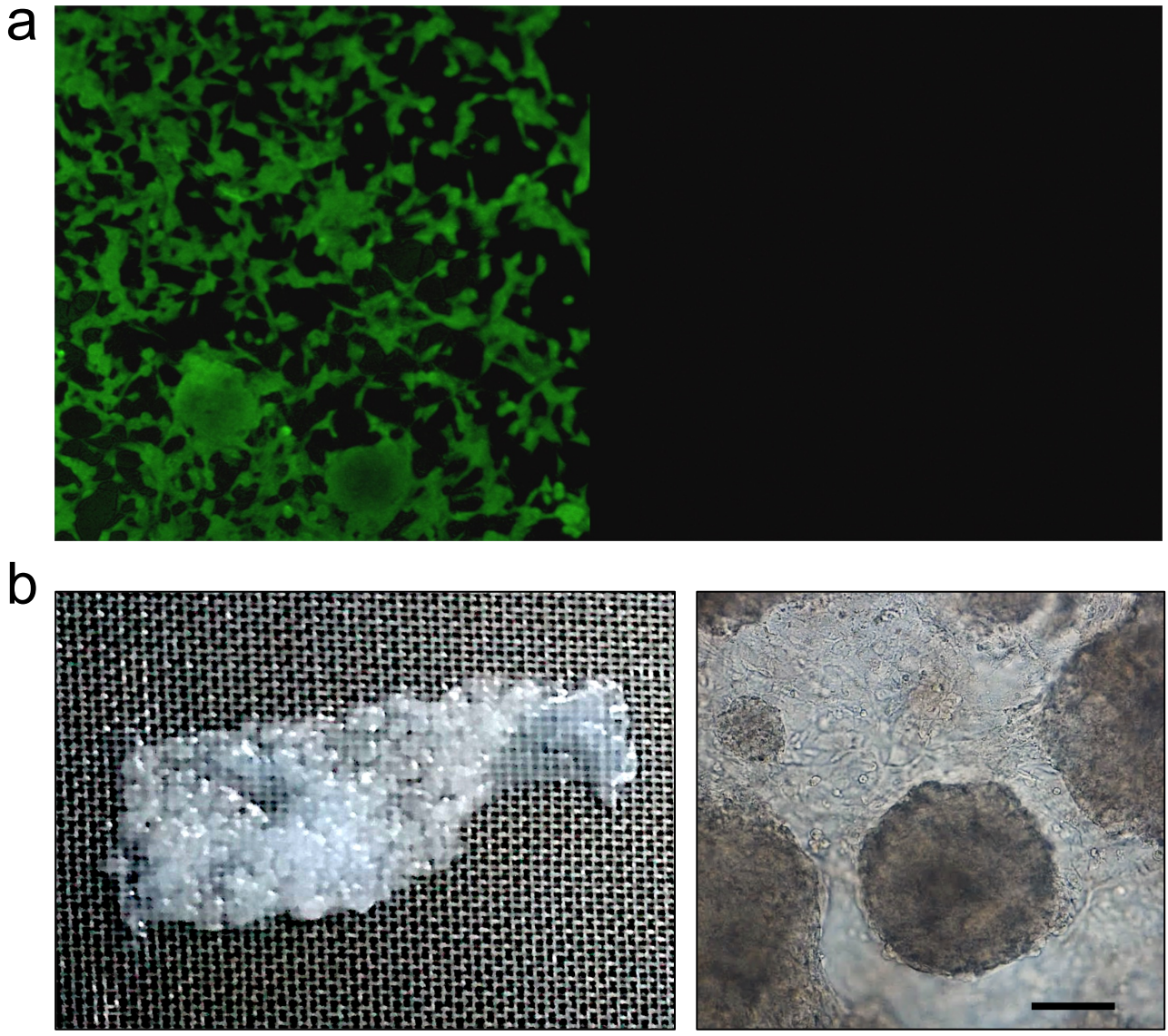


**Figure S1.**
**(a)** Confocal images of the perfused TE-NB model (top view) co-stained with the LIVE/DEAD® viability/cytotoxicity assay. Calcein-AM staining (left) show viable cells and EthD-1 staining (right) show the potential dead cells (EthD-1 positive cells were not detected).
**(b)** Macroscopic (left; top view) and microscopic (right) analyses of tumor aggregates generated within the perfused TE-NB model after 4 days of incubation in the perfusion bioreactor. (Scale bar: 100 µm).

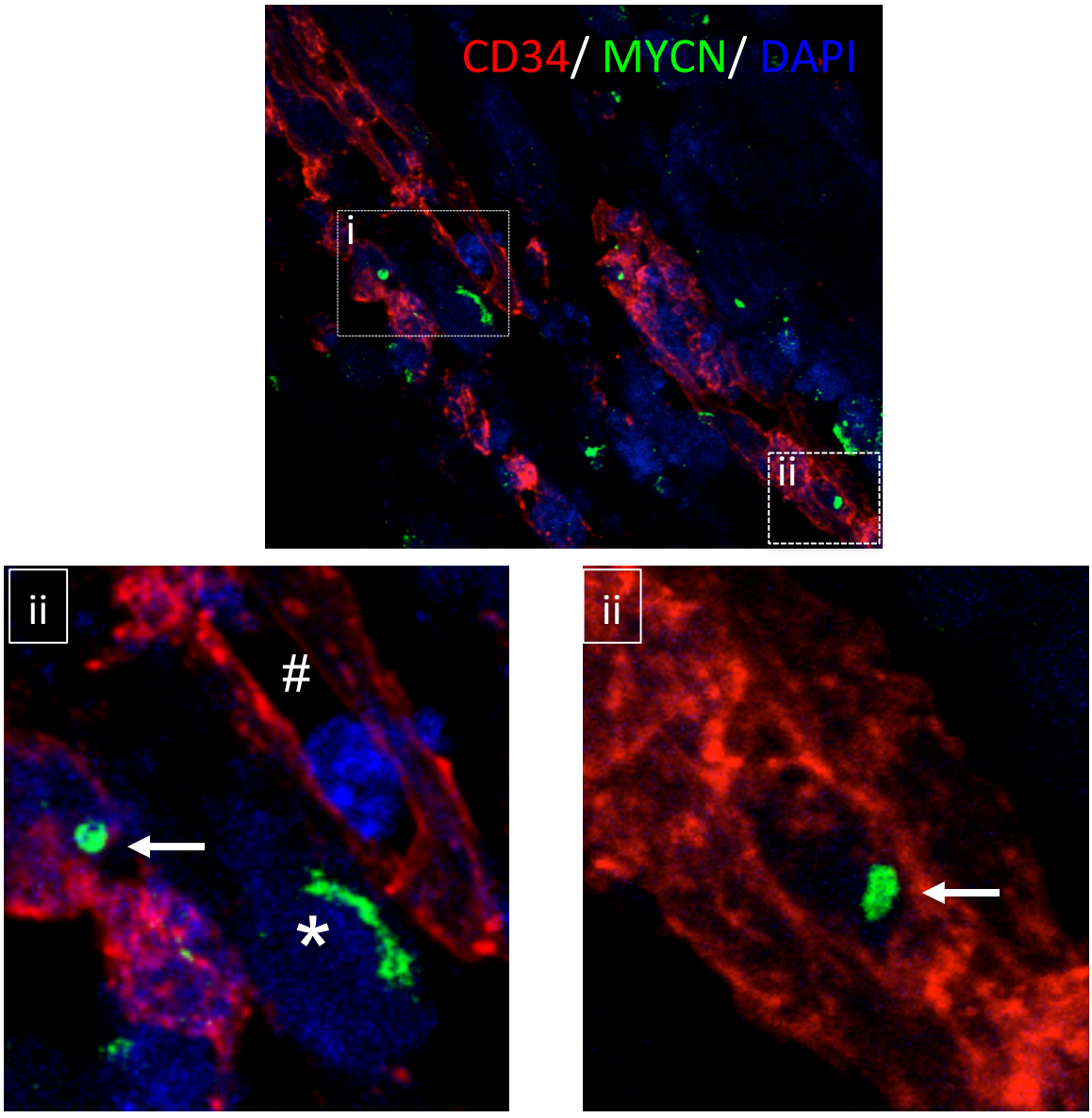


\# =HUVEC (MYCN negative and CD34 positive)
* = NB cell (MYCN positive and CD34 negative)
⟵ =TEC cell (MYCN positive and CD34 positive = Transdifferentiated NB cell

**Figure S2.** Representative Immunofluorescence images for the in situ localization of tumor-derived endothelial cells (TECs) by CD34/MYCN double staining. (i)TE-NB paraffin sections were stained with antibodies against CD31 (red) and MYCN (green). Nuclei were stained with DAPI(blue). (ii) and (iii) TEC were detected as double positive cells expressing MYCN and CD34 (white arrows), HUVECs (#; CD34 only positive cells) and neuroblastoma cells (*, NB cells- MYCN only) were also observed and clearly distinguished from TECs. (n=3)

a

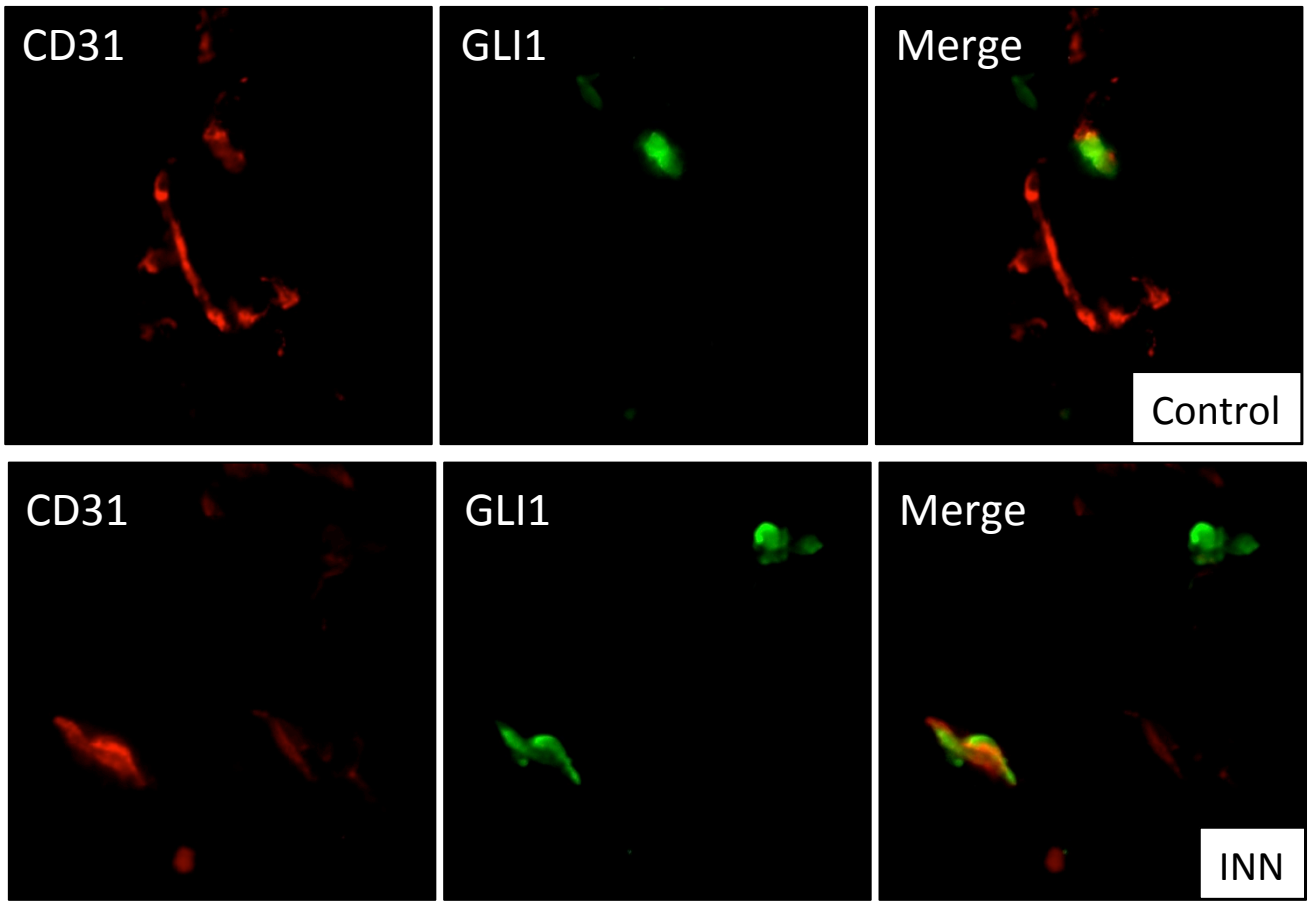
CD31
GLI1
Merge
Control
CD31
GLI1
Merge
INN

b

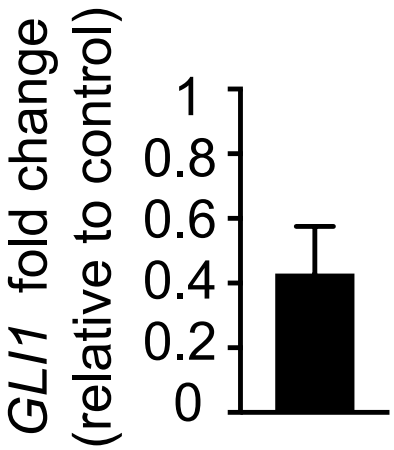
GLI1 fold change
(relative to control)
1
0.8
0.6
0.4
0.2
0

**Figure S3. GLI1 studies**

**(a)** Representative Immunofluorescence images for the in situ localization of tumor-derived endothelial cells (TECs) by CD31/ GLI1 double staining. TE-NB paraffin sections obtained from TE-NB controls and INN treated were stained with antibodies against CD31 (red) and GLI1 (green). TEC were observed as double positive cells expressing MYCN and CD31. (n=3)

**(b)** GLI1 levels determined by qRT-PCR. Fold change in GLI1 expression in tumor models treated with isotretinoin, as compared to untreated control tumor models. Relative endogenous expression of GLI1 was normalized to GAPDH; error bars represent standard deviation of relative expression. (control; n=3. INN; n=3)

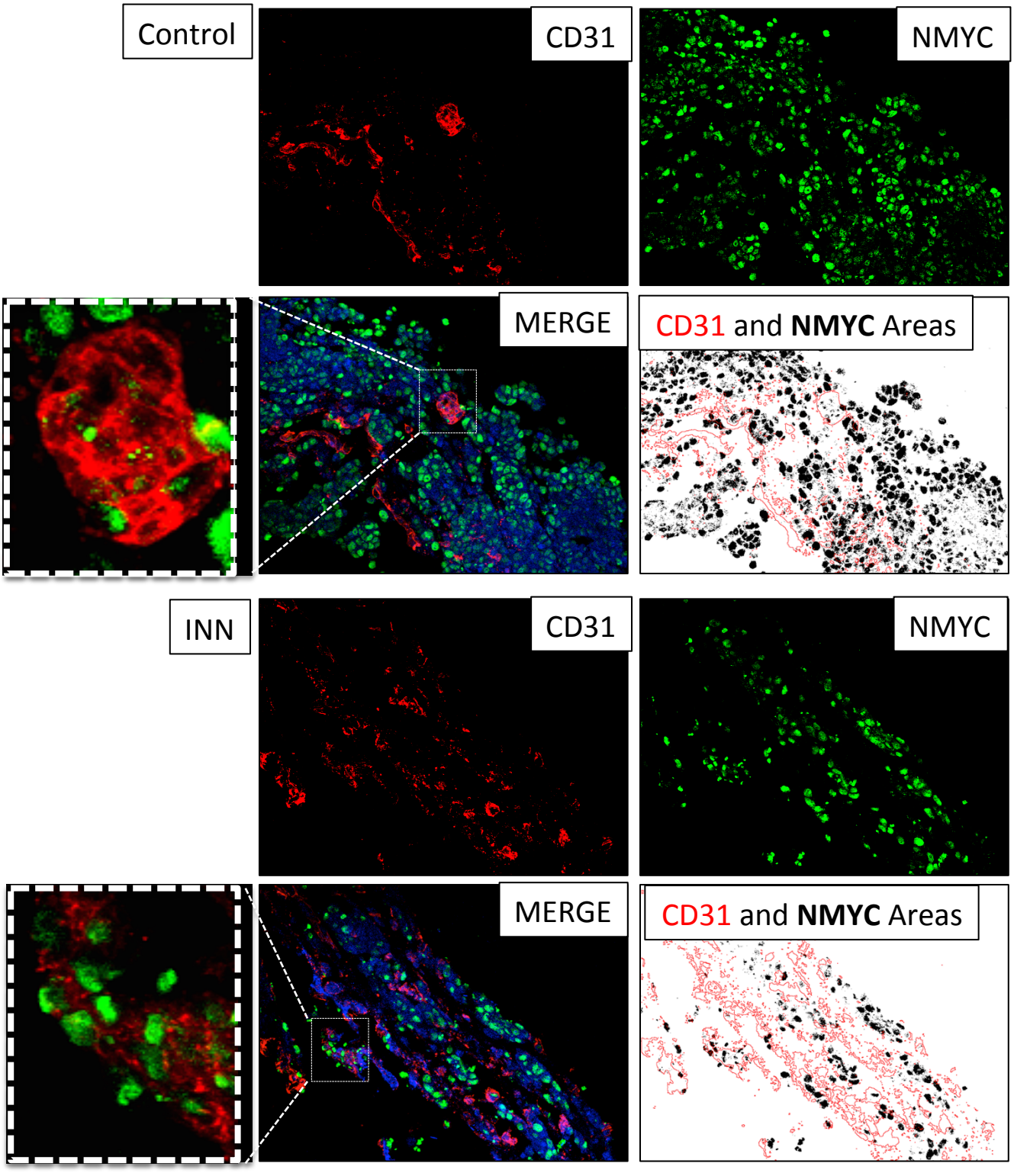


**Figure S4.** NMYC/CD31 co-localization maps (CD31 areas in red and NMYC areas in black) generated using imageJ (bottom right) from confocal stacked images of NMYC/CD31 double-stained samples in TE-BE models untreated (control; n=3) or treated with INN (INN; n=3), at day 5.

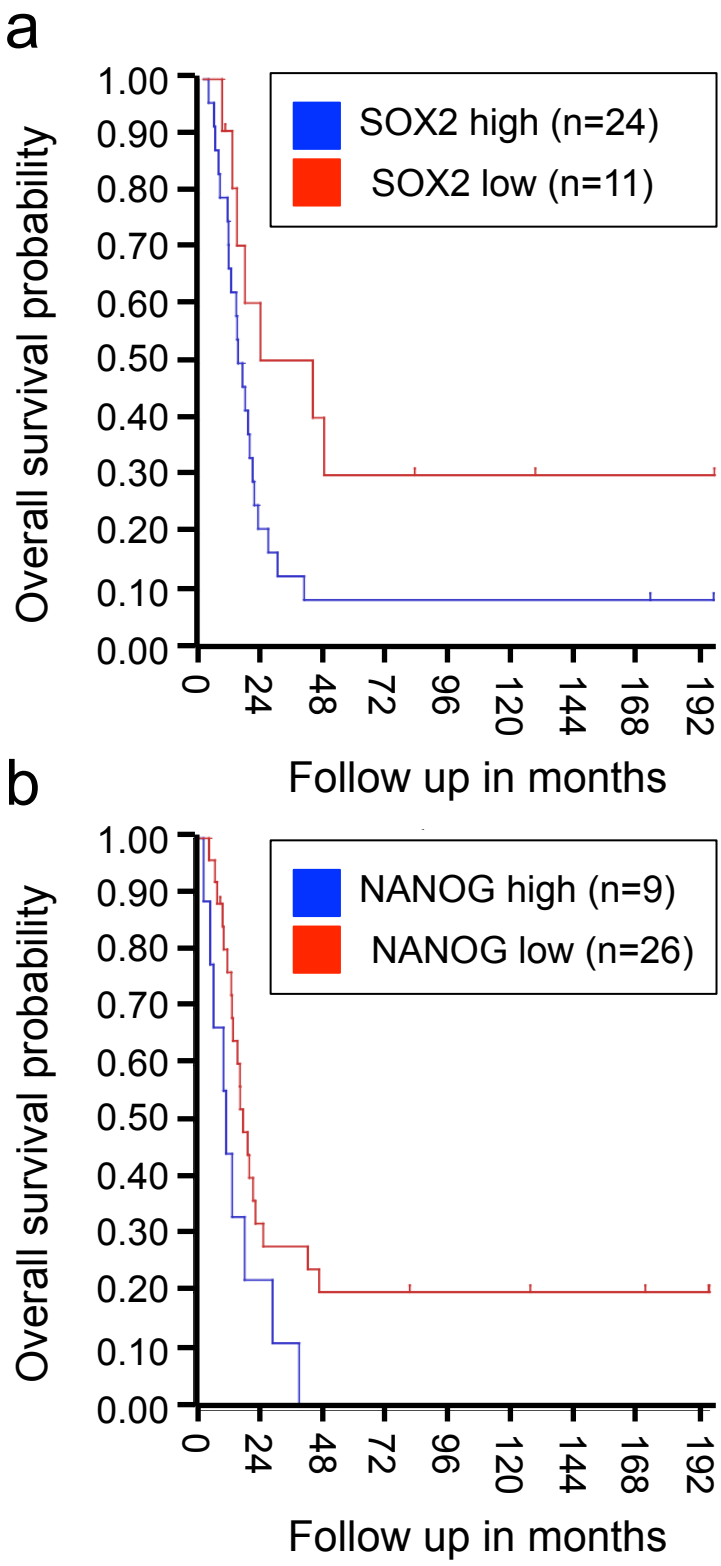


**Figure S5.** Overall survival probability of Neuroblastoma patients correlated with low or high levels of expression of the stemness genes **(a)** SOX2 and **(b)** NANOG obtained from public available expression array data (www.amc.com). Kaplan Meier analyses were performed using the R2 Genomics Analysis and Visualization Platform. The number of samples in each condition (low or high levels) is given.

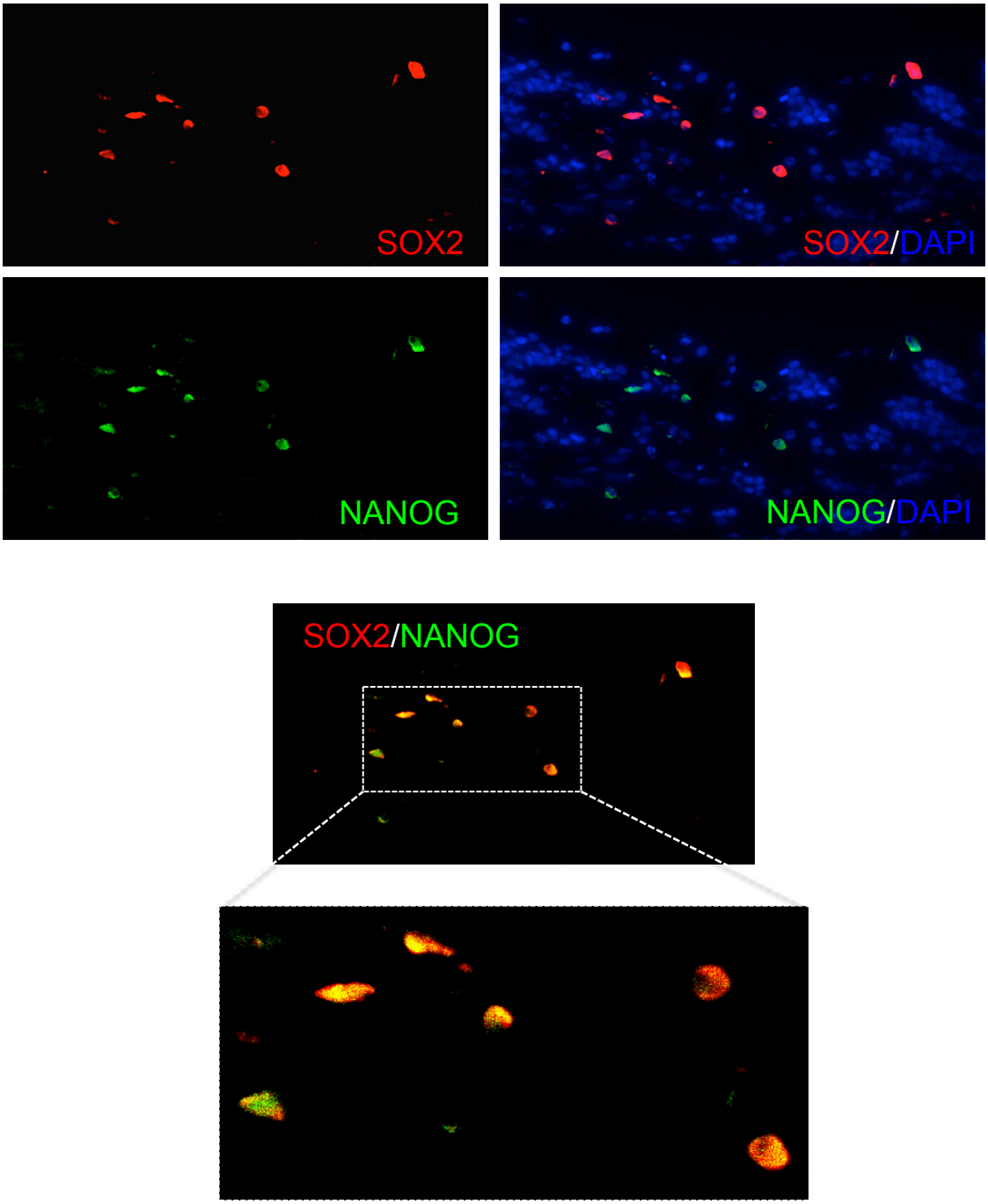


**Figure S6. Co-localization of SOX2 and NANOG analysis.** Representative Immunofluorescence images for detection of cancer stem-like cells (CSLC) in the TE-NB control model by SOX2/NANOG double staining. TE-NB paraffin sections were stained with antibodies against SOX2 (red) and NANOG (green). Nuclei were stained with DAPI(blue). CSLC were detected as double positive cells and SOX2 and NANOG co-localized in the nuclei of CSLC (TE-NB controls n=3).

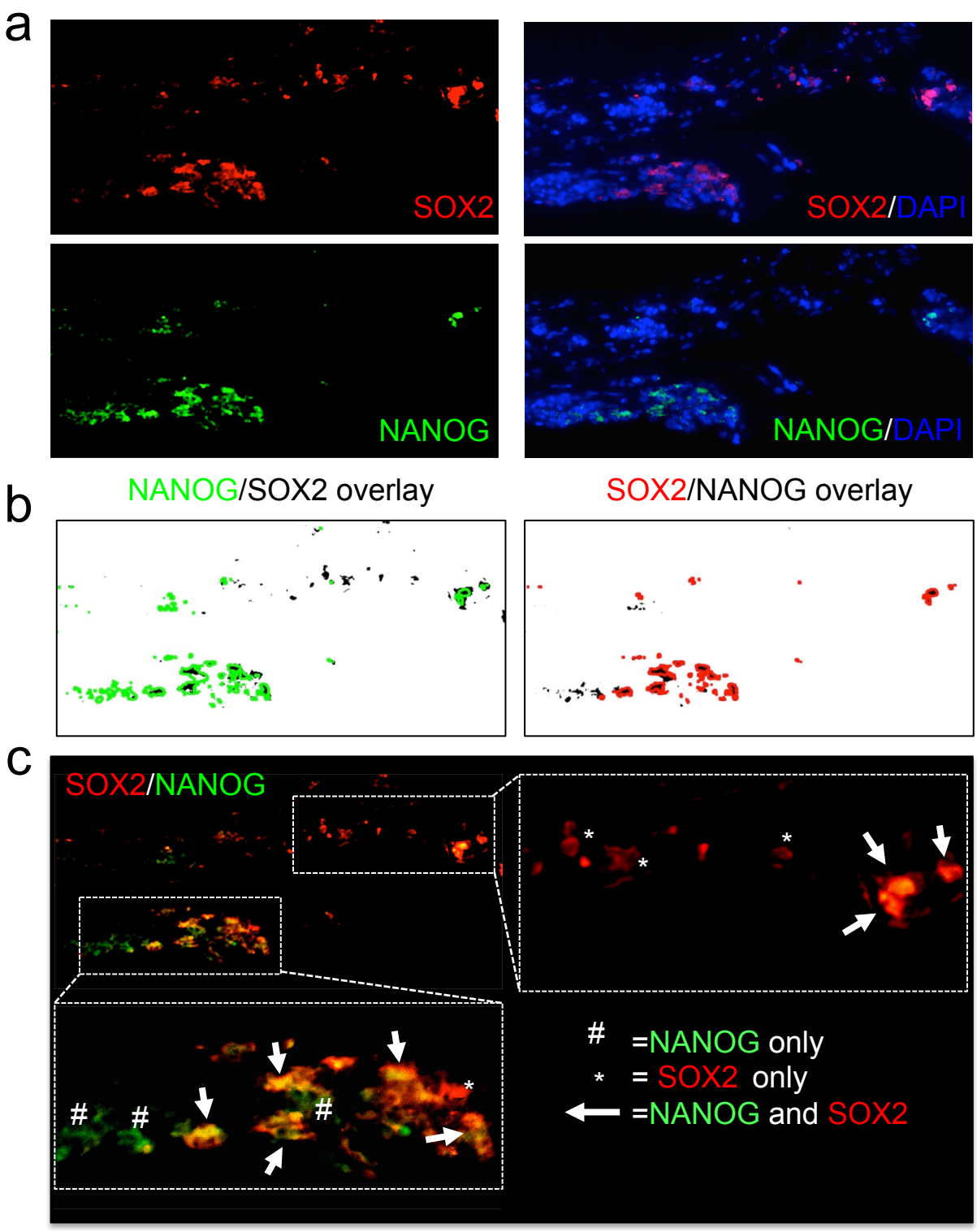


**Figure S7. Analysis of INN effect on SOX2 and NANOG co-localization. (a)** Representative Immunofluorescence of INN-treated TE-NB paraffin sections stained with antibodies against SOX2 (red) and NANOG (green). Nuclei were stained with DAPI(blue). **(b)** Co-localization maps of cells expressing SOX2 and NANOG generated by ImageJ. (left) Nanog positive areas (green) overlaid with SOX2 positive areas (black); and (right) SOX2 positive areas (red) overlaid with NANOG positive areas (black). **(c)** Merged immunofluorescence image showing heterogeneity within CSLC expressing NANOG and SOX2. (INN treated samples n=3).

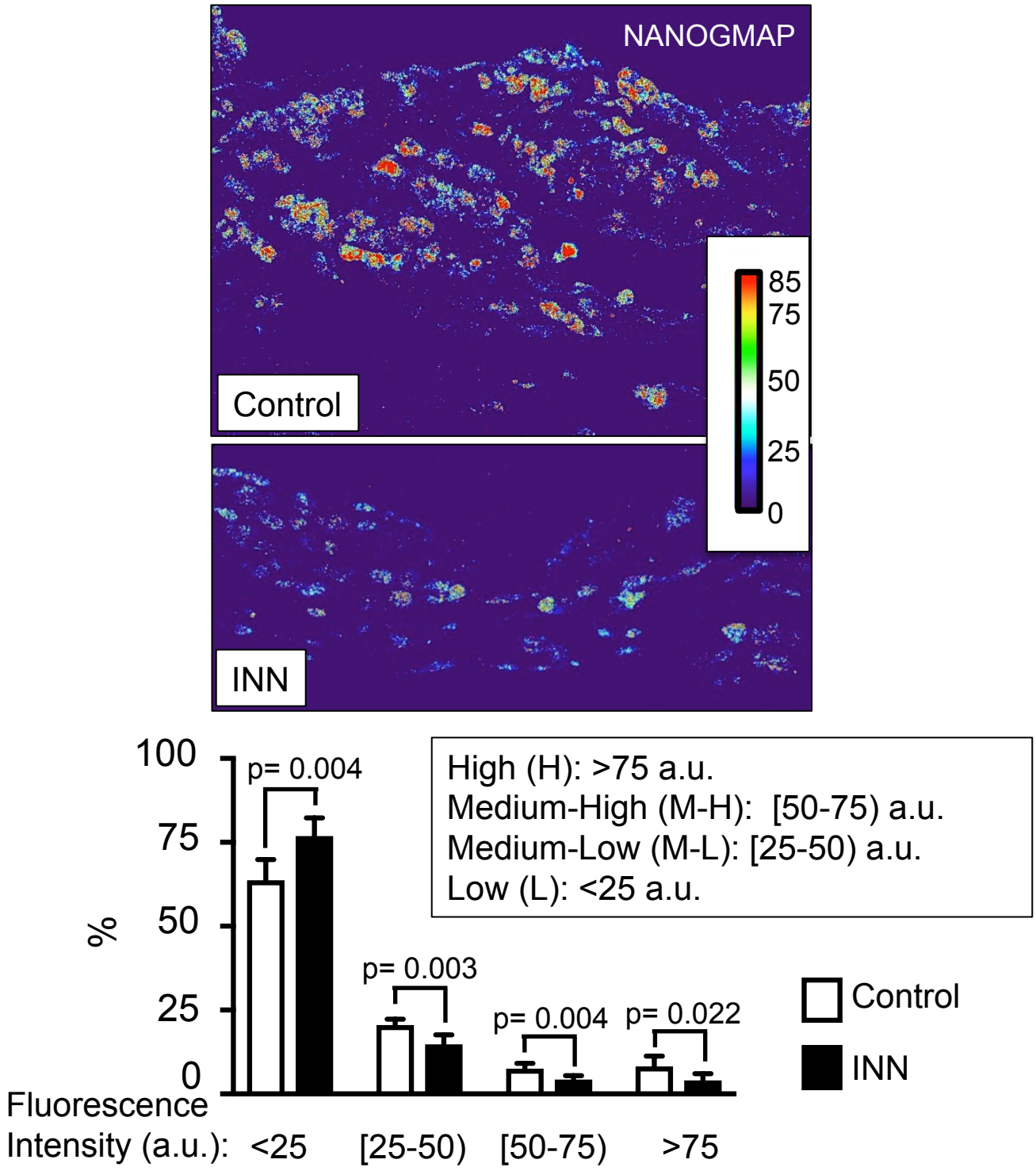


**Figure S8.** (top) Heatmaps of expression of NANOG (NANOGMAP) generated by applying ImageJ's Thermal LUT to confocal immunofluorescence stacked images stained for NANOG. Four categories according to NANOG fluorescence levels (colored as indicated in the scale bar and expressed in arbitrary units; a.u) were established (low, medium-low, medium-high and high levels of expression). (bottom) NANOGMAPs quantification of control and INN treated samples by ImageJ to obtain the percentage of NANOG levels in each category. Error bars represent standard deviations (n=3 for each group). Statistical significance was determined by the two- tailed Student's t test.

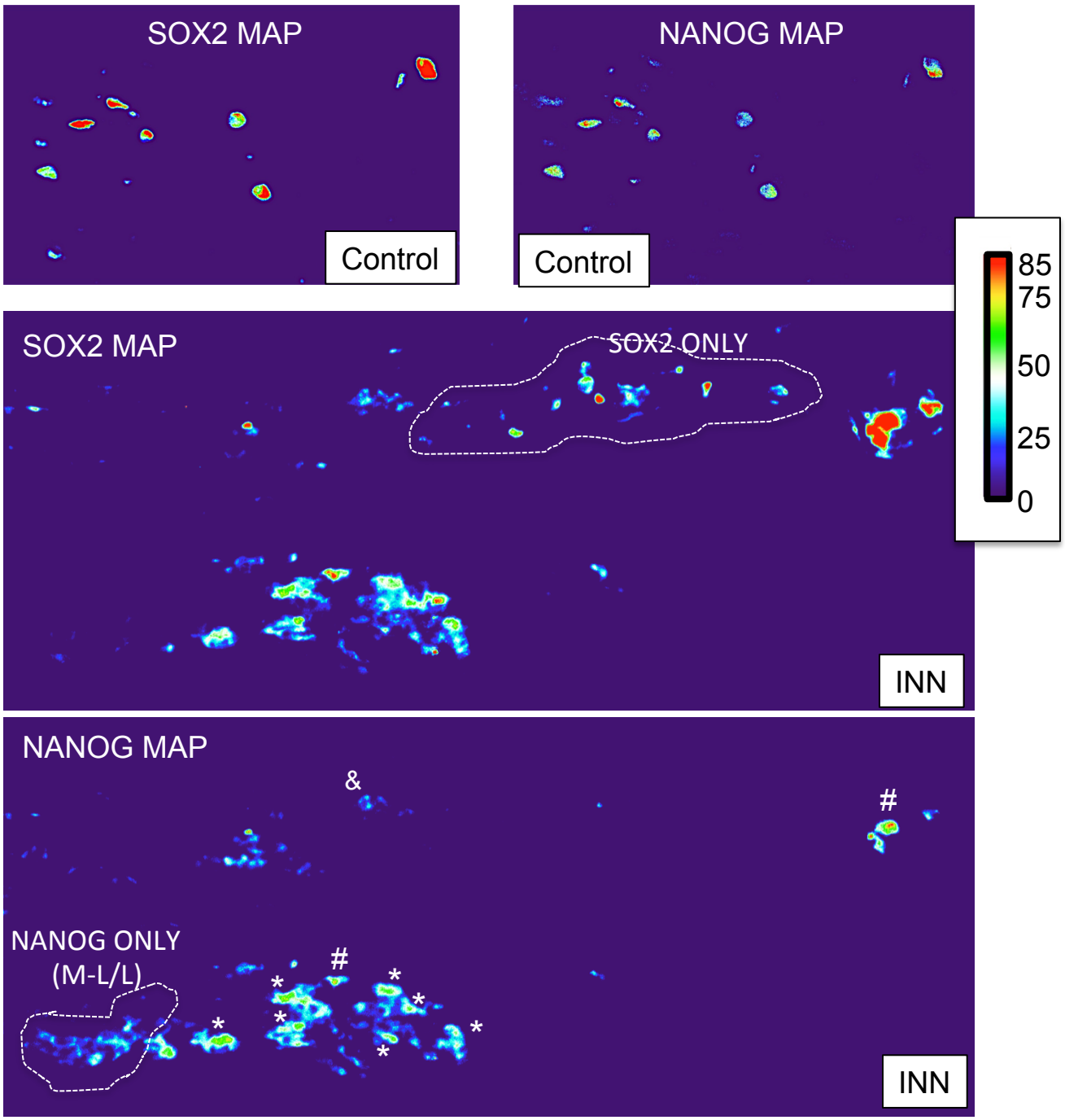


| | |
|---|---|
| High (H): >75 a.u. | # =High NANOG/SOX2 |
| Medium-High (M-H): [50-75) a.u. | * =M-H NANOG/SOX2 |
| Medium-Low (M-L): [25-50) a.u. | & =M-L NANOG/SOX2 |
| Low (L): <25 a.u. | |

**Figure S9.** Heatmaps of expression of SOX2 (SOX2 MAP) and NANOG (NANOG MAP) generated by applying ImageJ's Thermal LUT to confocal immunofluorescence stacked images stained for both SOX2 and NANOG. Four categories according to fluorescence levels (colored as indicated in the scale bar and expressed in arbitrary units; a.u) were established (low, medium-low, medium-high and high levels of expression).

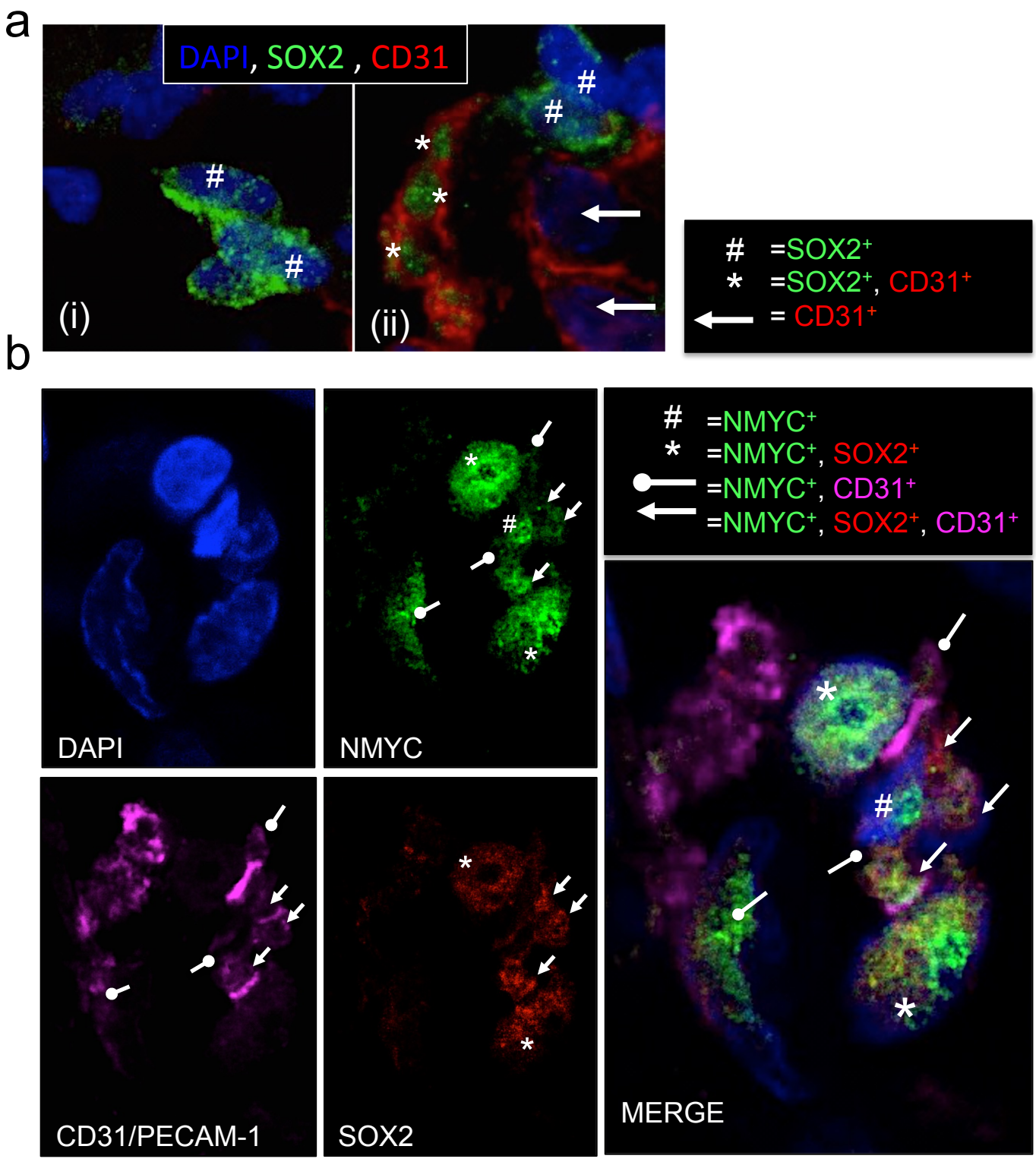


**Figure S10.** Confocal images of TE-BE samples treated with INN (n=3) showing cell heterogeneity. (a) Immunofluorescence staining of both SOX2 (green) and CD31 (red); (a.i) detail of cells expressing only SOX2 but not CD31 and (a.ii) expressing both markers. (b) Representative confocal image of a remaining vessel after INN treatment, which is stained for NMYC (green; NB cells),SOX2 (red, stemness marker) and CD31 (magenta, endothelial cell marker). NB cells (NMYC positive) can express SOX2 and CD31 at the same time. Nuclei are stained with DAPI (blue).